

# Silicon-Based Integrated Tunable Fractional Order Photonic Temporal Differentiators

Weilin Liu, *Student Member, IEEE*, Weifeng Zhang, *Student Member, IEEE*,  
and Jianping Yao, *Fellow, IEEE, Fellow, OSA*

**Abstract**—Two integrated fractional-order photonic temporal differentiators based on two Mach-Zehnder interferometer (MZI) structures implemented on a silicon-on-insulator (SOI) platform are designed, fabricated, and experimentally evaluated. The first photonic temporal differentiator employs a multimode interference (MMI) coupler as one of the two 3-dB couplers of the MZI. By changing the polarization state of the input optical signal, the coupling coefficient of the MMI is changed, which leads to the change of the phase shift in the destructive interference wavelength, and a photonic temporal differentiator with a tunable fractional order is implemented. The second photonic temporal differentiator is designed to have two cascaded MZIs, a balanced MZI, and an unbalanced MZI. A phase modulator (PM) is incorporated in one of the two arms of each of the MZIs. The balanced MZI with a PM forms an active tunable coupler, which is used to actively tune the fractional order of the temporal differentiator. The PM in the unbalanced MZI is used to tune the operating wavelength. The two photonic temporal differentiators are designed and fabricated in a CMOS compatible SOI platform, and their performance is evaluated experimentally. The experimental results show that both temporal differentiators can have a tunable fractional order from 0 to 1. In addition, the use of the active temporal differentiator to perform high-speed coding with a data rate of 16 Gb/s is experimentally evaluated.

**Index Terms**—Modulation coding, optical differentiator, silicon-on-insulator, silicon photonics.

## I. INTRODUCTION

A PHOTONIC temporal differentiator [1] is a device that performs the temporal differentiation of an optical signal, which can find important applications such as all-optical Fourier transform [2], [3], temporal pulse characterization [4], and optical demultiplexing of an optical time division multiplexed (OTDM) signal [5]. In general, a photonic temporal differentiator can have an  $n$ -th order that performs the  $n$ -th order time derivative of the complex envelope of an optical signal. For  $n = 1$ , the photonic temporal differentiator is a standard 1<sup>st</sup> order photonic temporal differentiator.

Manuscript received August 31, 2016; revised February 26, 2017 and March 21, 2017; accepted March 26, 2017. Date of publication March 27, 2017; date of current version May 5, 2017. This work was supported by the Natural Sciences and Engineering Research Council of Canada. (*Corresponding Author: Jianping Yao.*)

The authors are with Microwave Photonics Research Laboratory, School of Electrical Engineering and Computer Science, University of Ottawa, Ottawa, ON K1N 6N5, Canada (e-mail: jpyao@eecs.uottawa.ca).

Color versions of one or more of the figures in this paper are available online at <http://ieeexplore.ieee.org>.

Digital Object Identifier 10.1109/JLT.2017.2688468

To date, numerous techniques have been proposed to implement a photonic temporal differentiator, which can be classified into three categories. The first is to design a fiber Bragg grating (FBG) with a spectral response corresponding to that of a photonic temporal differentiator, the second is to use an optical ring resonator to implement a photonic temporal differentiator, and the third is to implement a photonic temporal differentiator based on an optical interferometer such as a Michelson or Mach-Zehnder interferometer (MZI).

In the first category, a photonic temporal differentiator is implemented by using an FBG in transmission which is designed based on a spectral-domain design approach. The transmission spectral response of an FBG can be designed to have a spectral response closely matched to that of a target differentiator by controlling the grating period, the apodization profile, or by introducing a  $\pi$  phase shift to the FBG. For example, a long-period fiber grating (LPFG) working in the linear regime inherently behaves as an ultrafast optical temporal differentiator [6], and the output temporal waveform in the core mode of an LPFG is proportional to the first derivative of the input optical temporal signal. The direct differentiation of a temporal waveform in the sub-picosecond regime using an LPFG was demonstrated [7]. By applying apodization in the fabrication of a linearly chirped FBG (LCFBG), an arbitrary order temporal differentiator can also be implemented with a bandwidth of a few hundreds of GHz [8], and the operating wavelength and bandwidth can also be tuned by packaging the LCFBG in a digitally controlled thermal print head [9]. In addition to the use of an FBG in transmission, a photonic temporal differentiator can also be implemented by an asymmetrical  $\pi$  phase-shifted FBG in reflection [10]. The main advantage of using a phase-shifted FBG as a differentiator is the relatively short grating length, which could be easily implemented in a photonic integrated platform, such as a sidewall phase-shifted Bragg grating in a silicon-on-insulator (SOI) platform [11]. The main limitation of the approaches in this category is that the differentiation order is difficult to tune.

In the second category, an optical microring resonator is used to implement a photonic temporal differentiator. The spectral response of a microring resonator has a notch at a resonant wavelength, which can be used to mimic a photonic differentiator. By tuning the coupling coefficient between the bus waveguide and the ring resonator, the phase change at the resonant wavelength can be changed, which would lead to a tunable fractional order of a photonic temporal differentiator implemented

by a ring resonator. In [12], a multimode interference (MMI) coupler was incorporated a ring resonator to achieve a tunable fractional order by changing the polarization state of the input optical signal. However, the processing bandwidth of the photonic temporal differentiator implemented by a microring resonator is limited as the notch bandwidth of a ring resonator is usually small.

In the third category, a photonic temporal differentiator is implemented by a conventional two-arm interferometer based on the spectral domain design approach. A conventional interferometer, such as a Michelson interferometer or an MZI, can provide a spectral response that is required for the implementation of first-order temporal differentiation over a certain bandwidth at a destructive-interference wavelength [13]. In this implementation, both the operation wavelength and bandwidth of the differentiator can be independently tuned by adjusting the relative time delay between the two arms. In addition, a tunable fractional order differentiator can be achieved by tuning the coupling coefficient of the input or output coupler in the interferometer. The implementation can also be transferred into an SOI platform to improve the compactness, cost, and robustness [14]. However, the lack of high speed tuning in this design limits its applications for high-speed reconfigurable signal processing.

In this paper, we propose two photonic integrated tunable fractional order photonic temporal differentiators based on MZI structures implemented in a CMOS compatible SOI platform, with the tuning of the fractional order achieved based on a passive or active design. In the passive design, an MMI is used as one of the two couplers in the MZI. By changing the polarization state of the input signal, the coupling coefficient of the MMI can be tuned [12]. Correspondingly, the phase shift in the destructive-interference wavelength is changed, which leads to a tunable fractional order of the photonic temporal differentiator. In the active design, the photonic temporal differentiator uses two cascaded MZIs, a balanced MZI and an unbalanced MZI. A phase modulator (PM) is incorporated in one of the two arms of each MZI, as a result, the balanced MZI with a PM forms a tunable coupler, which is used to tune the fractional order of the active differentiator. The PM in the unbalanced MZI is used to tune the operation wavelength. The two photonic temporal differentiators are designed and fabricated in a CMOS compatible SOI platform, and their performance is evaluated experimentally. The experimental results show that both differentiators can have a tunable fractional order from 0 to 1. In addition, the use of the active temporal differentiator to perform high speed coding with a data rate of 16 Gbps is also experimentally evaluated.

The paper is organized as follows. In Section II, the principle of a photonic temporal differentiator based on an MZI is presented, with an emphasis on the passive and active designs on a CMOS compatible SOI platform. In Section III, the fabrication results of the proposed passive and active designs are given, and an experimental demonstration for photonic temporal differentiation using the fabricated devices is presented. A high speed coding system based on the active photonic temporal differentiator with a data rate of 16 Gbps is also demonstrated. A conclusion is drawn in Section IV.

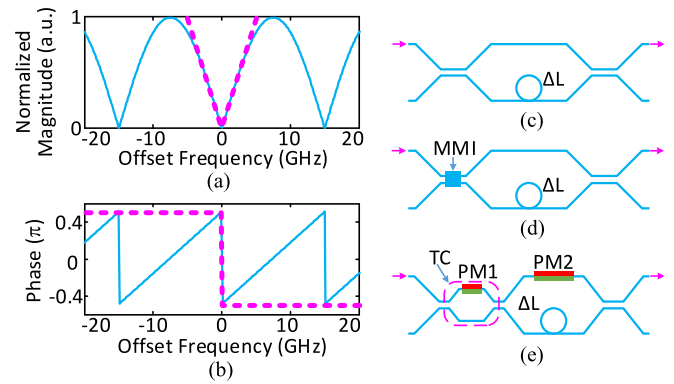


Fig. 1. (a) The magnitude and (b) phase responses of an MZI (solid line) and an ideal photonic temporal differentiator (dashed line). (c) An MZI with a length difference  $\Delta L$  between the two arms. (d) The passive and (e) active design concept of a tunable fractional photonic temporal differentiator based on an SOI MZI. MMI: multimode interference; PM: phase modulator; TC: tunable coupler.

## II. PRINCIPLE

An  $n$ -th order temporal differentiator is a device that performs the  $n$ -th order time derivative of the envelope of an optical signal. An  $n$ -th order temporal differentiator can be considered as an LTI system with a transfer function given by

$$H_n(\omega) = [j(\omega - \omega_0)]^n \quad (1)$$

$$= \begin{cases} e^{jn\pi/2} |\omega - \omega_0|^n, & \omega > \omega_0 \\ e^{-jn\pi/2} |\omega - \omega_0|^n, & \omega < \omega_0 \end{cases} \quad (2)$$

where  $j = \sqrt{-1}$ ,  $\omega$  is the optical angular frequency,  $\omega_0$  is the carrier angular frequency of the signal to be processed, and the order  $n$  can be a positive integer or a fraction. As can be seen an  $n$ -th order temporal differentiator has a magnitude response of  $|\omega - \omega_0|^n$  and a phase shift of  $n\pi$  at  $\omega_0$ , as shown in Fig. 1(a) and (b) (dashed lines) with an order  $n = 1$ . An optical filter with a frequency response given by (1) can be implemented by an MZI, shown in Fig. 1(c) [13], [15], which has a magnitude and phase response that is close to that of an ideal temporal differentiator, as shown in Fig. 1(a) and (b) (solid lines).

To achieve a tunable fractional order in a photonic temporal differentiator, a tunable coupler has to be used as one of the two couplers in the MZI to achieve a tunable phase shift at a destructive-interference wavelength. In a CMOS compatible SOI platform, a tunable coupler can be implemented by a 2-D grating coupler and a  $2 \times 2$  MMI in the passive approach as shown in Fig. 1(d) or by an MZI coupler with a PM in one of its two arms in an active approach as shown in Fig. 1(e).

The passive approach is simple and easy to achieve at a fixed operating wavelength, but a polarization controller at the input is required to tune the fraction order and the tuning speed is slow. The active approach can provide a much faster tuning speed, but a PM in the tunable MZI coupler is needed, which is more complicated than the passive approach. In addition, the operating wavelength is tunable by incorporating a PM in one of the main MZI arms. The comparison between the two approaches provides a reference for the design of a SOI photonic temporal differentiator to meet different applications needs. For

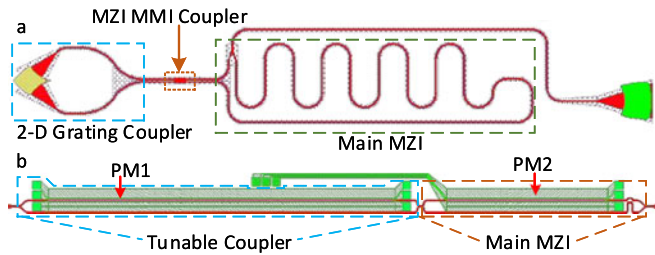


Fig. 2. (a) The design layout of the proposed passive photonic temporal differentiator based on an MZI with an MMI coupler. The length difference between the two MZI arms is  $\Delta L = 780 \mu\text{m}$ . (b) The design layout of the active photonic temporal differentiator based on two cascaded MZIs with a PM in one of the two arms for each MZI. The PM is designed with a PN junction. The length difference between the two MZI arms for the two designs is  $\Delta L = 160 \mu\text{m}$ .

low cost and low speed applications, the passive approach can be used. The active approach can be used for applications where tunable operating wavelength and fast tuning speed are needed.

The design of a photonic temporal differentiator based on an MZI in a passive SOI platform is given in Fig. 2(a). A 2-D grating coupler supporting two orthogonally polarized optical fiber modes is used to couple an optical signal from a cleaved optical fiber into the chip. The 2-D grating coupler is a standard library element from the IMEC process design kit (PDK), which couples two orthogonally and linearly polarized modes in an optical fiber into two silicon waveguides [16]. The 2-D grating has a period of 605 nm, and the circular holes have a diameter of 390 nm. The waveguides of the fiber coupler are etched through the silicon top layer, but the grating holes are only etched 70 nm deep. The 3-dB bandwidth of the 2-D grating coupler is  $\sim 60 \text{ nm}$  with a central wavelength of 1545 nm, and the minimum insertion loss is 6.7 dB [17]. The first coupler in the MZI is implemented by a  $2 \times 2$  MMI with a dimension of  $7.5 \mu\text{m} \times 3 \mu\text{m}$  to provide a 3 dB power splitting ratio for a TE input optical signal. By changing the polarization state of the input optical signal, the coupling coefficient of the MMI can be tuned, which provides a phase shift change in the destructive-interference wavelengths and leads to a tunable fractional order of the photonic temporal differentiator. The length difference between the two MZI arms is  $780 \mu\text{m}$  which corresponds to a free spectral range (FSR) of  $\sim 110 \text{ GHz}$  in the frequency response of the MZI. With such a compact design, the footprint of the passive photonic differentiator has a dimension of  $450 \mu\text{m} \times 65 \mu\text{m}$ . The tuning of the fractional order is achieved by adjusting the polarization state of the input optical signal, and the operation wavelength is not tunable.

The design of a photonic temporal differentiator based on an MZI in an active SOI platform is given in Fig. 2(b). As shown in Fig. 2(b), a tunable coupler implemented by an MZI with a PM (PM1) with a length of  $8.1 \mu\text{m}$  in one of its two arms is used as the first coupler in the main MZI. The PM is implemented by a PN junction in the SOI platform, which has a bandwidth of  $\sim 25 \text{ GHz}$  with a length of 4 mm. By applying a DC voltage or a coding signal to PM1, the coupling coefficient of the tunable coupler can be changed, which leads to the tuning of the fractional order. Followed by the tunable coupler, the two arms of the main MZI has a length difference of  $500 \mu\text{m}$ , which corresponds to a FSR

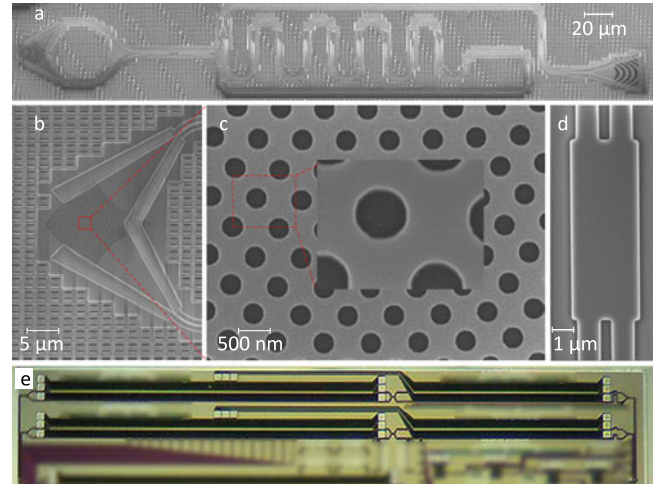


Fig. 3. Fabrication results. (a) SEM pictures of the fabricated passive photonic temporal differentiator based on an MZI, (b) the 2-D grating coupler, (c) the zoom-in view of the 2-D grating coupler, and (d) the MMI with an actual fabricated dimension of  $8.130 \mu\text{m} \times 3.088 \mu\text{m}$ . (e) The microscopic view of the fabricated active photonic temporal differentiator.

of  $\sim 170 \text{ GHz}$  in the frequency response of the MZI. A second PM (PM2) with a length of 2.3 mm is also incorporated in one of the two arms of the main MZI to provide a tunable operation wavelength for the photonic temporal differentiator. A grating coupler is used to couple optical signal from a cleaved optical fiber into the chip and a second grating coupler is used to couple the differentiated optical signal out of the chip. Due to the large size of the PMs used in the design, the footprint of such an active photonic temporal differentiator has a dimension of  $0.32 \text{ mm} \times 7.7 \text{ mm}$ .

The design of a passive photonic differentiator based on an MZI has a very compact footprint, but the tuning speed of the fraction order is limited since the tuning is done by changing the polarization state of the input optical signal, and the operation wavelength is not tunable. The design of an active photonic differentiator, on the other hand, has a much high speed for fractional order tuning and the operation wavelength can also be tunable. But the footprint is much larger due to the use of two PMs, which usually have a large size.

### III. EXPERIMENT

The proposed photonic temporal differentiators, as shown in Fig. 2, are fabricated using a CMOS compatible process with 193-nm deep ultraviolet lithography. The strip waveguides in the device have a width of 500 nm and a height of 220 nm, which are fabricated on top of a buried oxide layer ( $2 \mu\text{m}$  thick) on a silicon wafer. Fig. 3 presents the SEM and microscopic pictures of the fabricated devices. Specifically, Fig. 3(a) shows a passive photonic temporal differentiator. The 2-D grating coupler is shown in Fig. 3(b) and (c), and the fabricated MMI is shown in Fig. 3(d), which has a dimension of  $8.130 \mu\text{m} \times 3.088 \mu\text{m}$ , with a size that matches closely to the design dimension of  $7.5 \mu\text{m} \times 3 \mu\text{m}$ . Fig. 3(e) shows the fabricated active photonic temporal differentiator.

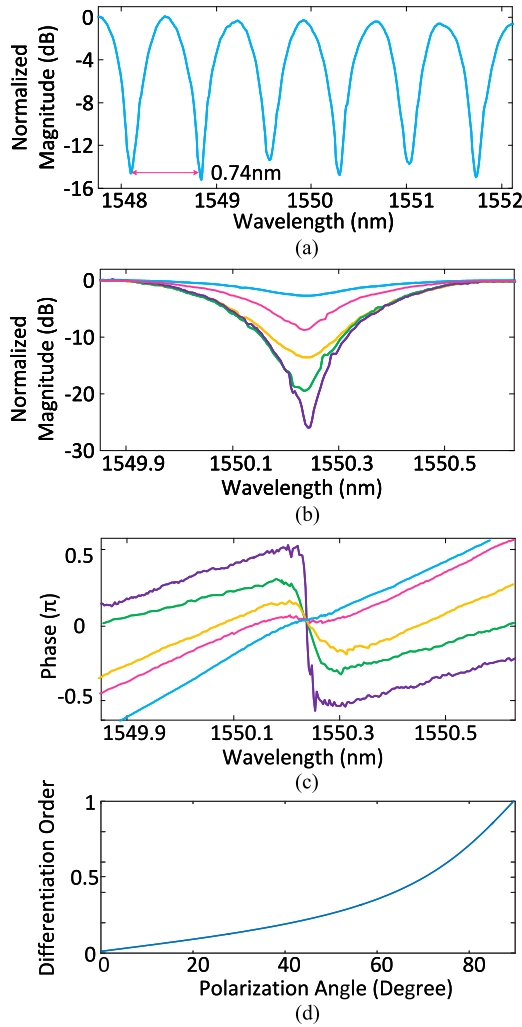


Fig. 4. Experimental results of the passive photonic temporal differentiator. (a) The spectral response of the of the MZI photonic temporal differentiator. (b) The spectral response and (c) phase response of the differentiator when tuning the polarization state of the input optical signal. (d) Simulation results to show the differentiation order as a function of the state of polarization of the input optical light.

#### A. Photonic Temporal Differentiation Results Based on the Passive Design

An experiment to measure and demonstrate the fabricated passive photonic temporal differentiator is implemented. The spectral response of the differentiator is firstly measured by an optical vector analyzer (OVA, Luna), as shown in Fig. 4(a). As can be seen, the measured FSR is 0.74 nm (or 92.4 GHz), which is the maximum processing bandwidth of the differentiator. By changing the polarization state of the input optical signal, the spectral response and phase shift at the destructive-interference wavelength are changed, as shown in Fig. 4(b) and (c). This is also confirmed by a simulation, as shown in Fig. 4(d). As can be seen when the polarization state of the input optical signal is changed, the tunable differentiation order is changed.

An optical Gaussian pulse train generated by a mode-locked laser (MLL, Pritel 1550-nm Picosecond and Femtosecond Fiber Lasers) with a pulse width of 11.8 ps and a repetition rate of

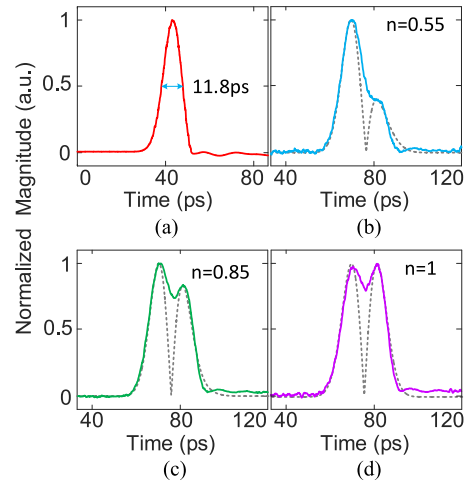


Fig. 5. Experimental results of the passive photonic temporal differentiator. (a) The input Gaussian pulse with a temporal width of 11.8 ps. The measured (solid) and simulated (dashed) fractional differentiation of the input Gaussian pulse with a fractional order of (b) 0.55, (c) 0.85, and (d) 1.

40 MHz is sent to the passive differentiator through a polarization controller (PC). Fig. 5(a) shows a single Gaussian pulse in the pulse train. By controlling the polarization state of the input Gaussian pulse, a temporal differentiated pulse with a tunable fractional order is obtained. To observe the differentiated pulse, the optical signal at the output of the on-chip differentiator is applied to a 53-GHz photodetector (PD) and monitored by a sampling oscilloscope (OSC, Agilent 86100C). Fig. 5(b)–(d) shows the differentiated pulse with a fractional order of 0.55, 0.85, and 1, respectively. Simulation results of an ideal differentiator are also given in Fig. 5(b)–(d) (dashed lines). As can be seen, the experimental results have a good agreement with the simulated results. It should be noted that the difference in the notch between experimental and simulation results is caused mainly by the limited bandwidth of the PD (53 GHz), and the difference in the tail is due to the non-ideal Gaussian profile of the input pulse as shown in Fig. 5(a).

#### B. Photonic Temporal Differentiation Results Based on the Active Design

An experiment to measure and demonstrate the fabricated active photonic temporal differentiator is also implemented. The spectral responses of the active differentiator while applying a voltage of  $-1$ ,  $-2$ , and  $-3$  V to the PM in the second MZI (PM2), as shown in Fig. 1(e), are measured by an optical vector analyzer (OVA, Luna Technologies), as shown in Fig. 6(a). As can be seen, the measured FSR is 1.37 nm (or 171.1 GHz), which is the maximum processing bandwidth of the differentiator. By changing the voltage applied to the PM in the first MZI (PM1), the spectral response and phase shift at the destructive-interference wavelength are changed, as shown in Fig. 6(b) and (c). The voltages applied to PM1 are 0, 1, 2, 3.5, and 5 V, corresponding to a fractional order of 0, 0.16, 0.41, 0.60, and 1, respectively. The 3-dB bandwidths of PM1 and PM2 are also measured, which are 24.2 GHz and 5 GHz, respectively.

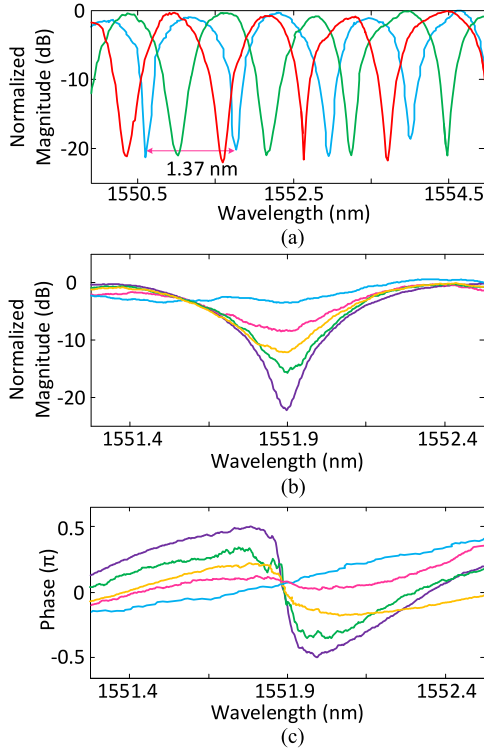


Fig. 6. Experimental results of the active photonic temporal differentiator. (a) The spectral response of the of the MZI photonic temporal differentiator when applying three different voltages to the PM in the second MZI. (b) The spectral response and (c) phase response of the differentiator when the voltage to the PM in the first MZI is tuned at five different values.

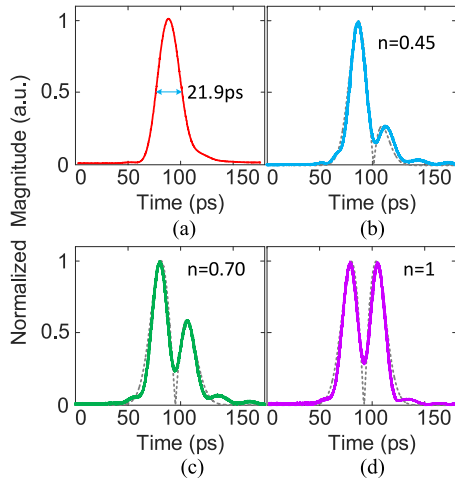


Fig. 7. Experimental results of the active photonic temporal differentiator. (a) The input Gaussian pulse with a temporal width of 21.9 ps. The measured (solid) and simulated (dashed) fractional differentiator of the input Gaussian pulse with a fractional order of (b) 0.45, (c) 0.70, and (d) 1.

An optical Gaussian pulse train generated by an MLL (Pritel 1550-nm Picosecond and Femtosecond Fiber Lasers) with a pulse width of 21.9 ps and a repetition rate of 40 MHz is sent to the active photonic temporal differentiator through a PC, as shown in Fig. 7(a). By changing the voltage applied to PM1, temporally differentiated pulses with a fractional order of

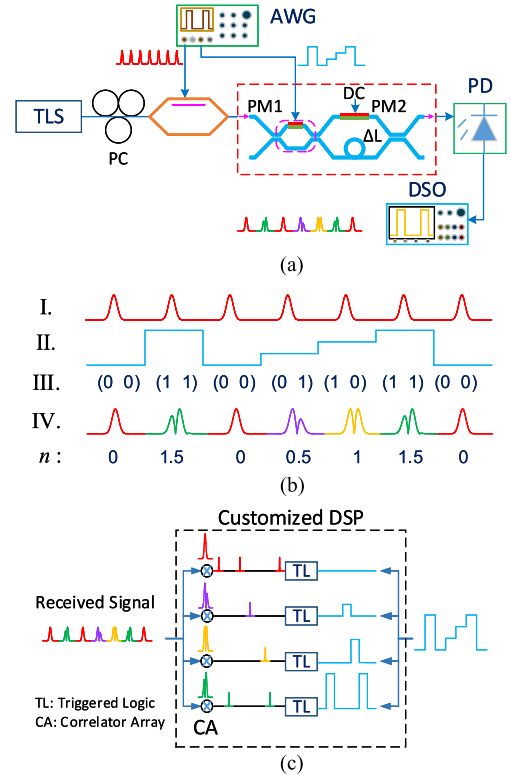


Fig. 8. (a) Schematic of a high speed coding system based on the active photonic temporal differentiator. (b) The coding map of the proposed high speed coding system with (I) a Gaussian pulse train, (II) a 4-level data sequence, (III) a mapping 2-bit data sequence, and (IV) the coded differentiation pulse train. (c) The diagram of a digital decoding receiver.

0.45, 0.70, and 1 are obtained, which are detected by using a 53-GHz PD and observed by an OSC (Agilent 86100C), as shown in Fig. 7(b)–(d), respectively. Simulation results of an ideal photonic temporal differentiator are also given in Fig. 7(b)–(d) (dashed lines). As can be seen, the experimental results have a good agreement with the simulated results except some small difference in notch depth. It should be noted that the small difference in the notch depth between the experimentally generated and simulated pulses are also resulted from the limited bandwidth of the PD, which has a bandwidth of 53 GHz.

### C. High Speed Coding Based on the Active Photonic Temporal Differentiator

As shown in Fig. 7, a tunable fraction order photonic temporal differentiator can shape a Gaussian pulse into a differentiated pulse with a tunable fractional order. Therefore, a high speed coding system can be implemented based on such a differentiator, in which the coding can be done by applying a coding signal to PM1, as shown in Fig. 8(a). Fig. 8(b) shows the coding map. To represent a 2-bit data sequence, a Gaussian pulse train can be differentiated with a fractional order of 0, 0.5, 1, and 1.5 by applying a 4-level data sequence to PM1. As shown in Fig. 8(a), a continuous wave (CW) light wave with a wavelength of 1551.9 nm is generated by a tunable laser source (TLS, Ag-

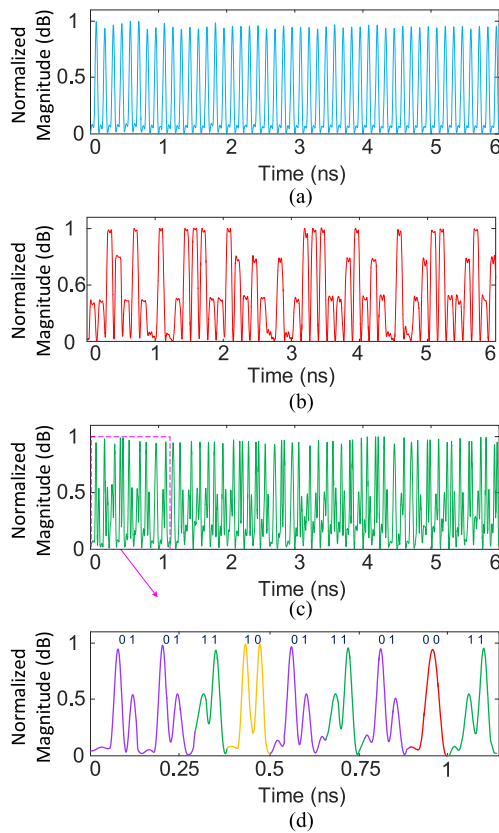


Fig. 9. Experimental results of high speed coding based on the active photonic differentiator. (a) The Gaussian pulse train with a repetition rate of 8 GHz. (b) The synchronized 4-level data sequence used for high speed coding. (c) The generated differentiation pulse train with coded data. (d) A close view of the generated pulse train shown in (c).

ilent N7714A) and sent to a Mach-Zehnder modulator (MZM) through a PC. The light wave is modulated by an electric Gaussian pulse train with a repetition rate of 8 GHz generated by an arbitrary waveform generator (AWG, Keysight M8195A) as shown in Fig. 9(a). The modulated light wave is then sent to the active photonic temporal differentiator by a cleaved optical fiber through a grating coupler. A synchronized 4-level data sequence generated by the AWG, as shown in Fig. 9(b), is applied to PM1 in the differentiator with a controllable DC bias by a bias tee. A coded pulse train is obtained at the output of the differentiator, which is monitored by a digital storage oscilloscope (DSO, Agilent DSO-X 93204A), as shown in Fig. 9(c). A close view of the coded pulse train from in a 1 ns scale is also shown in Fig. 9(d). As can be seen, the proposed active photonic temporal differentiator can be used for high speed coding with a data rate of 16 Gbps. As the decoding of the differentiated data sequence can only be successful by performing correlation between the encoded signal and a signature sequence with the coding map [18], [19], thus this approach can find important applications in secure communications. A high-speed modulator (PM1) is used in this design, by which secure communications at a speed up to tens of Gbps can be achieved.

To decode the received signal, the correlation between the received encoded signal and a signature sequence is required,

which can be performed by an analog correlator or a digital correlator. For the use of an analog correlator, sampling before decoding is not needed, however, sampling and digitization are required if digital processing for correlation is used. For example, the decoding process based on correlation can be performed in a customized digital signal processor (DSP) as shown Fig. 8(c). The digitized received signal is equally split into four sub-signal sequences. For each of the sub-signal sequence, a correlation is performed between the sub-signal sequence and one of the four signature signals, which are determined in the transmitter when the signal is generated and encoded. After the correlation, the four signature signals are found in the four sub-signal sequences with each having a correlation peak. The correlation peaks can be converted into multilevel voltage signals by triggered logics, which can be combined into a sequence of multilevel voltage signal. In this way, the encoded signal can be successfully decoded. Those processes can be implemented in a customized DSP for real time decoding processing.

#### IV. CONCLUSION

We have designed, fabricated and experimentally evaluated two integrated fractional-order photonic temporal differentiators based on MZI structures implemented on a SOI platform, with passive and active tuning of the fractional orders. In the design of the passive fractional-order photonic temporal differentiator, an MMI was incorporated into the MZI as one of the two couplers. A tunable fractional order from 0 to 1 was achieved by changing the polarization state of the input optical signal. In the design of the active fractional-order photonic temporal differentiator, two cascaded MZIs were used with each having a PM in one arm to achieve active fractional order and wavelength tuning. The tunable fractional order and the tunable operation frequency were achieved by changing the voltage applied to the two PMs (PM1 and PM2). In the experiment demonstration, for both differentiators the differentiation of a Gaussian pulse with a pulse width of 21.9 ps was achieved with a fractional order from 0 to 1. The active photonic temporal differentiator was also evaluated for its use for high speed coding. In the experiment, a coding signal with a data rate of 16 Gbps was generated. The coding system can find important applications in secure communications.

#### ACKNOWLEDGMENT

The authors would like to thank CMC Microsystems for providing the design tools and enabling the fabrication of the device.

#### REFERENCES

- [1] F. Liu *et al.*, "Compact optical temporal differentiator based on silicon microring resonator," *Opt. Express*, vol. 16, no. 20, pp. 15880–15886, Sep. 2008.
- [2] D. Hillerkuss *et al.*, "Simple all-optical FFT scheme enabling Tbit/s real-time signal processing," *Opt. Express*, vol. 18, no. 9, pp. 9324–9340, Apr. 2010.
- [3] D. Hillerkuss *et al.*, "26 Tbit s<sup>-1</sup> line-rate super-channel transmission utilizing all-optical fast Fourier transform processing," *Nature Photon.*, vol. 5, no. 6, pp. 364–371, May 2011.

- [4] F. Li, Y. Park, and J. Azaña, "Complete temporal pulse characterization based on phase reconstruction using optical ultrafast differentiation (PROUD)," *Opt. Express*, vol. 32, no. 22, pp. 3364–3366, Nov. 2007.
- [5] R. Slavík *et al.*, "Demultiplexing of 320 Gbit/s OTDM data using ultrashort flat-top pulses," *IEEE Photon. Technol. Lett.*, vol. 19, no. 22, pp. 1855–1857, Nov. 2007.
- [6] M. Kulishov and J. Azaña, "Long-period fiber gratings as ultrafast optical differentiators," *Opt. Lett.*, vol. 30, no. 20, pp. 2700–2702, Oct. 2005.
- [7] R. Slavík, Y. Park, M. Kulishov, R. Morandotti, and J. Azaña, "Ultrafast all optical differentiators," *Opt. Express*, vol. 14, no. 22, pp. 10699–10707, Oct. 2006.
- [8] L. M. Rivas, K. Singh, A. Carballar, and J. Azaña, "Arbitrary-order ultra-broadband all-optical differentiators based on fiber Bragg gratings," *IEEE Photon. Technol. Lett.*, vol. 19, no. 16, pp. 1209–1211, Aug. 2007.
- [9] R. Wang *et al.*, "Electrically programmable all-fiber structured second order optical temporal differentiator," *IEEE Photon. J.*, vol. 7, no. 3, Apr. 2015, Art. no. 7101510.
- [10] C. Cuadrado-Laborde and M. V. Andrés, "In-fiber all-optical fractional differentiator," *Opt. Lett.*, vol. 34, no. 6, pp. 833–835, Mar. 2009.
- [11] W. Zhang, W. Li, and J. P. Yao, "Optical differentiator based on an integrated sidewall phase-shifted Bragg grating," *IEEE Photon. Technol. Lett.*, vol. 26, no. 23, pp. 2383–2386, Dec. 2014.
- [12] H. Shahoei, D. Xu, J. Schmid, and J. P. Yao, "Photonic fractional-order differentiator using an SOI microring resonator with an MMI coupler," *IEEE Photon. Technol. Lett.*, vol. 25, no. 15, pp. 1408–1411, Aug. 2013.
- [13] Y. Park, J. Azaña, and R. Slavík, "Ultrafast all-optical first- and higher-order differentiators based on interferometers," *Opt. Lett.*, vol. 32, no. 6, pp. 710–712, Mar. 2007.
- [14] J. Dong, A. Zheng, D. Gao, L. Li, D. Huang, and X. Zhang, "Compact, flexible and versatile photonic differentiator using silicon Mach-Zehnder interferometers," *Opt. Express*, vol. 21, no. 6, pp. 7014–7024, Mar. 2013.
- [15] W. Liu *et al.*, "A fully reconfigurable photonic integrated signal processor," *Nature Photon.*, vol. 10, no. 3, pp. 190–195, Mar. 2016.
- [16] W. Bogaerts, D. Taillaert, P. Dumon, D. Van Thourhout, R. Baets, and E. Pluk, "A polarization-diversity wavelength duplexer circuit in silicon-on-insulator photonic wires," *Opt. Express*, vol. 15, no. 4, pp. 1567–1578, Feb. 2007.
- [17] S. Pathak, M. Vanslebrouck, P. Dumon, D. Van Thourhout, and W. Bogaerts, "Compact SOI-based polarization diversity wavelength demultiplexer circuit using two symmetric AWGs," *Opt. Express*, vol. 20, no. 26, pp. B493–B500, Dec. 2012.
- [18] E. Hamidi and A. M. Weiner, "Phase-only matched filtering of ultrawideband arbitrary microwave waveforms via optical pulse shaping," *J. Lightw. Technol.*, vol. 26, no. 15, pp. 2355–2363, Aug. 2008.
- [19] I. S. Lin and A. M. Weiner, "Selective correlation detection of photonically generated ultrawideband RF signals," *J. Lightw. Technol.*, vol. 26, no. 15, pp. 2692–2699, Aug. 2008.

**Weilin Liu** (S'10) received the B.Eng. degree in electronic information engineering from the University of Science and Technology of China, Hefei, China, in 2009, and the M.A.Sc. degree in electrical and computer engineering in 2011 from the School of Electrical Engineering and Computer Science, University of Ottawa, Ottawa, ON, Canada, where he is currently working toward the Ph.D. degree in the Microwave Photonics Research Laboratory.

He is currently working in the Microwave Photonics Research Laboratory, School of Electrical Engineering and Computer Science, University of Ottawa His research interests include microwave/terahertz generation, optical signal processing, fiber Bragg grating, and their applications in microwave photonic systems.

**Weifeng Zhang** (S'12) received the B.Eng. degree in electronic science and technology from Xi'an Jiaotong University, Xi'an, China, in 2008, and the M.A.Sc. degree in electrical engineering from the Polytechnic University of Turin, Turin, Italy, in 2011. He is currently working toward the Ph.D. degree in electrical engineering at the Microwave Photonics Research Laboratory, School of Electrical Engineering and Computer Science, University of Ottawa, Ottawa, ON, Canada.

His current research interests include silicon photonics and its applications in microwave photonics.

**Jianping Yao** (M'99–SM'01–F'12) received the Ph.D. degree in electrical engineering from the Université de Toulon et du Var, Toulon, France, in December 1997.

He is currently a Professor and the University Research Chair in the School of Electrical Engineering and Computer Science, University of Ottawa, Ottawa, ON, Canada. From 1998 to 2001, he was with the School of Electrical and Electronic Engineering, Nanyang Technological University, Singapore, as an Assistant Professor. In December 2001, he joined the School of Electrical Engineering and Computer Science, University of Ottawa, as an Assistant Professor, where he was promoted to Associate Professor in 2003, and Full Professor in 2006. He has authored or coauthored more than 510 research papers, including more than 300 papers in peer-reviewed journals and 210 papers in conference proceedings. From July 2007 to June 2010 and July 2013 to June 2016, he was the Director of the Ottawa-Carleton Institute for Electrical and Computer Engineering.

Prof. Yao is a Topical Editor for *Optics Letters*, and serves on the Editorial Boards of the IEEE TRANSACTIONS ON MICROWAVE THEORY AND TECHNIQUES, *Optics Communications*, *Frontiers of Optoelectronics*, and *Science Bulletin*. He was as a Guest Co-Editor for a Focus Issue on microwave photonics in *Optics Express* in 2013 and a Lead-Editor for a Feature Issue on microwave photonics in *Photonics Research* in 2014. He is a Chair of numerous international conferences, symposia, and workshops, including the University Research Chair in Microwave Photonics in 2007, the Vice Technical Program Committee (TPC) Chair of the IEEE Microwave Photonics Conference in 2007, the TPC Co-Chair of the Asia-Pacific Microwave Photonics Conference in 2009 and 2010, the TPC Chair of the high-speed and broadband wireless technologies subcommittee of the IEEE Radio Wireless Symposium in 2009–2012, the TPC Chair of the microwave photonics subcommittee of the IEEE Photonics Society Annual Meeting in 2009, the TPC Chair of the IEEE Microwave Photonics Conference in 2010, the General Co-Chair of the IEEE Microwave Photonics Conference in 2011, the TPC Co-Chair of the IEEE Microwave Photonics Conference in 2014, and the General Co-Chair of the IEEE Microwave Photonics Conference in 2015. He is also a committee member of numerous international conferences, such as IPC, OFC, BGPP, and MWP. He received the 2005 International Creative Research Award of the University of Ottawa, the 2007 George S. Glinski Award for Excellence in Research, the Natural Sciences and Engineering Research Council of Canada Discovery Accelerator Supplements Award in 2008. He was selected to receive an inaugural OSA Outstanding Reviewer Award in 2012. He was the IEEE MTT-S Distinguished Microwave Lecturer for 2013–2015. He was conferred the title of Distinguished University Professor of the University of Ottawa in June 2016, and is also a registered Professional Engineer in Ontario. He is a Fellow of the Canadian Academy of Engineering.